CARRIER DIFFUSION DEGRADATION OF CCD (CHARGE-COUPLED DEVICES) IMAGER MTF (MODULATION TRANSFER FUNCTION) FOR BROADBAND OPTICAL SOURCES

David H. Seib

Aerospace Corporation

Prepared for:

Space and Missile Systems Organization

29 January 1976

REPORT SAMSO-TR-76-25

Carrier Diffusion Degradation of CCD Imager MTF for Broadband Optical Sources

D. H. SEIB
Electronics Research Laboratory
Laboratory Operations
The Aerospace Corporation
El Segundo, Calif. 90245

29 January 1976

Interim Report

APPROVED FOR PUBLIC RELEASE:
DISTRIBUTION UNLIMITED

Prepared for

SPACE AND MISSILE SYSTEMS ORGANIZATION
AIR FORCE SYSTEMS COMMAND
Los Angeles Air Force Station
P.O. Box 92960, Worldway Postal Center
Los Angeles, Calif. 90009

This report was submitted by The Aerospace Corporation, El Segundo, CA 90245, under Contract F04701-75-C-0076 with the Space and Missile Systems Organization, Deputy for Space Communications Systems, P.O. Box 92960, Worldway Postal Center, Los Angeles, CA 90009. It was reviewed and approved for The Aerospace Corporation by A. H. Silver, Director, Electronics Research Laboratory. Lt Ronald C. Lawson, SAMSO/DYN, was the project officer.

This report has been reviewed by the Information Office (OI) and is releasable to the National Technical Information Service (NTIS). At NTIS, it will be available to the general public, including foreign nations.

This technical report has been reviewed and is approved for publication. Publication of this report does not constitute Air Force approval of the report's findings or conclusions. It is published only for the exchange and stimulation of ideas.

FOR THE COMMANDER

Ronald C. Lawson

Ronald C. Lawson
2nd Lt, United States Air Force
Office of Research Applications
Deputy for Technology

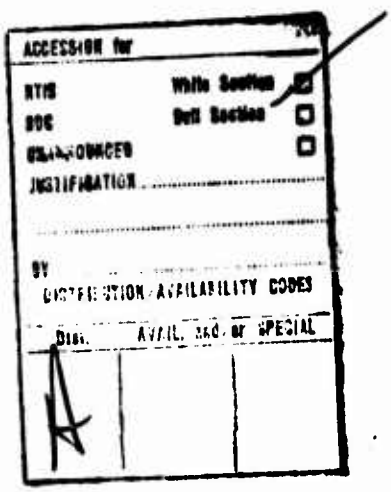

UNCLASSIFIED

SECURITY CLASSIFICATION OF THIS PAGE (When Data Entered)

REPORT DOCUMENTATION PAGE		READ INSTRUCTIONS BEFORE COMPLETING FORM
1. REPORT NUMBER SAMSO-TR-76-25	2. GOVT ACCESSION NO.	3. RECIPIENT'S CATALOG NUMBER
4. TITLE (and Subtitle) CARRIER DIFFUSION DEGRADATION OF CCD IMAGER MTF FOR BROADBAND OPTICAL SOURCES		5. TYPE OF REPORT & PERIOD COVERED Interim 6. PERFORMING ORG. REPORT NUMBER TR-0076(6930)-2
7. AUTHOR(s) David H. Seib		8. CONTRACT OR GRANT NUMBER(s) F04701-75-C-0076
9. PERFORMING ORGANIZATION NAME AND ADDRESS The Aerospace Corporation El Segundo, Calif. 90245		10. PROGRAM ELEMENT, PROJECT, TASK AREA & WORK UNIT NUMBERS
11. CONTROLLING OFFICE NAME AND ADDRESS Space and Missile Systems Organization Air Force Systems Command Los Angeles, Calif. 90009		12. REPORT DATE 29 January 1976 13. NUMBER OF PAGES ~~29~~ 30
14. MONITORING AGENCY NAME & ADDRESS(if different from Controlling Office)		15. SECURITY CLASS. (of this report) Unclassified 15a. DECLASSIFICATION/DOWNGRADING SCHEDULE

16. DISTRIBUTION STATEMENT (of this Report)

Approved for public release; distribution unlimited

17. DISTRIBUTION STATEMENT (of the abstract entered in Block 20, if different from Report)

18. SUPPLEMENTARY NOTES

19. KEY WORDS (Continue on reverse side if necessary and identify by block number)

Charge-Coupled Imagers
Charge-Coupled Devices
Modulation Transfer Function
Solid State Imaging Devices

20. ABSTRACT (Continue on reverse side if necessary and identify by block number)

Analytical results for the degradation of charge-coupled-imager modulation transfer function due to minority carrier diffusion effects are given for broadband optical sources. Both frontside and backside illuminated devices are considered. The effect of restricting the optical band on both broadband modulation transfer function and responsivity is considered. It is concluded that best imager performance is obtained for the full optical band (0.4-1.2 μm), and that backside illumination is the best approach to device

DD FORM 1473 (FACSIMILE)

UNCLASSIFIED

SECURITY CLASSIFICATION OF THIS PAGE (When Data Entered)

19. KEY WORDS *(Continued)*

20. ABSTRACT *(Continued)*

fabrication from the standpoint of carrier diffusion degradation of modulation transfer function.

CONTENTS

FIGURES

FIGURES (Continued)

I. INTRODUCTION

In a previous paper (Ref. 1) the degradation of modulation transfer function (MTF) due to carrier diffusion effects in charge-coupled imagers (CCI's) was considered for monochromatic optical inputs. In this report, these analytical results are extended to encompass broadband optical input sources. This extension is of obvious importance since most CCI applications involve broadband sources. The calculations to be presented are intended to facilitate comparison of theory with experimental measurements of CCI MTF's, which are usually done with a band of wavelengths. The question of whether it is beneficial to filter out certain wavelengths to improve MTF is also addressed. Broadband MTF's for both frontside-illuminated and backside-illuminated CCI's are considered and compared, using typical, representative, parameter values. Since in frontside and backside illuminated imagers long and short wavelengths, respectively, contribute most to the degradation of MTF, appropriate optical filtering can be used to improve MTF. However, this improvement comes at the expense of broadband responsivity. Calculations are therefore given of the broadband responsivity for different optical bands as well as the broadband MTF in order to evaluate the tradeoff between MTF improvement and responsivity degradation.

II. THEORETICAL BACKGROUND

The monochromatic, carrier diffusion MTF for both frontside and backside illuminated CCI's was previously evaluated (Ref. 1) by solving the minority carrier diffusion equation with the uniform depletion approximation and appropriate boundary conditions (Ref. 2). Let the monochromatic MTF as a function of ν_s (spatial frequency in cycles/mm) and λ (optical wavelength) obtained in this way be MTF (ν_s, λ). The diffusion equation which determines MTF (ν_s, λ) is linear. Therefore, superposition holds, and the broadband MTF, $\overline{\text{MTF}}\,(\nu_s, \lambda_i, \lambda_f)$, due to excitation by a band of wavelengths extending from initial wavelength λ_i to final wavelength λ_f can be expressed as:

$$\overline{\text{MTF}}\,(\nu_s, \lambda_i, \lambda_f) = \frac{\int_{\lambda_i}^{\lambda_f} \eta(\lambda)\, N(\lambda)\, T(\lambda)\, \text{MTF}(\nu_s, \lambda)\, d\lambda}{\int_{\lambda_i}^{\lambda_f} \eta(\lambda)\, N(\lambda)\, T(\lambda)\, d\lambda} \qquad (1)$$

Here $N(\lambda)$ and $\eta(\lambda)$ are the number of photons incident on and the quantum efficiency of the CCI at λ. $T(\lambda)$ is the number of incident photons transmitted into the silicon; for backside illumination $T(\lambda)$ is $1.0 - R(\lambda)$ ($R(\lambda)$ = imager reflectivity), while for frontside illumination $T(\lambda)$ is the transmission of the multilayer interference filter formed by oxide and electrode layers. The inclusion of these terms properly normalizes $\overline{\text{MTF}}\,(\nu_s, \lambda_i, \lambda_f)$ to the number of photoelectrons collected due to source photons at wavelength λ. To obtain $N(\lambda)$, a black body source of specified temperature is assumed; calculations are given for source temperatures of 2854 K and 4800 K. $\eta(\lambda)$ is obtained from the diffusion model which determines MTF (ν_s, λ).

III. FRONTSIDE ILLUMINATION

For evaluation of $\overline{MTF}$ for both frontside and backside illuminated devices, the values of optical absorption constant, α, for silicon given by Eden (Ref. 3) are used. For a frontside illuminated device, the following parameters are chosen for use in calculations. The depletion width, W_D, is taken to be 4.0 μm; this is representative of widths which can be readily attained in practice (Ref. 4). Diffusion length is taken to be 100 μm. For $T(\lambda)$, the transmittance curve calculated by Brown and Chamberlain (Ref. 5) is used. This curve gives the transmittance of layers of pyroglass, polysilicon, and SiO_2 on silicon, and has been reproduced in Fig. 1. The curve was smoothly extrapolated to a value of ~20% at longer wavelengths. The use of a transmittance curve for a particular layer structure and set of layer thicknesses does not detract significantly from the generality of the results and conclusions presented below. This occurs because $T(\lambda)$ appears in an integral (Eq. (1)), making $\overline{MTF}$ relatively insensitive to the exact shape of $T(\lambda)$. Also, because $T(\lambda)$ is in both the numerator and denominator of Eq. (1), $\overline{MTF}$ is insensitive to the scale of $T(\lambda)$. The optical wavelength band is assumed to be limited by an ideal optical filter with unity transmission for $\lambda_i \leq \lambda \leq \lambda_f$ and zero otherwise.

There are three parameters in $\overline{MTF}$ $(\nu_s, \lambda_i, \lambda_f)$; therefore there are several ways to present the calculated results. One method is to fix the final wavelength, λ_f, at some value and display $\overline{MTF}$ as a function of ν_s with λ_i as a parameter. An example is shown in Fig. 2, where $\lambda_f = 1.2$ μm, $T_s = 2854$ K, and curves are shown for $\lambda_i = 0.5, 0.7, 0.9$ and 1.1 μm. Other parameters are as discussed above for the frontside illuminated imager. To read Fig. 2, locate the curve which corresponds to the initial wavelength of the spectral band of interest, remembering $\lambda_f = 1.2$ μm, and read $\overline{MTF}$ as a function of ν_s.

If the spectral band reaching the sensor is filtered to eliminate long wavelengths (toward the final wavelength end), a new set of curves corresponding to the new λ_f must be used. Curves for $\lambda_f = 0.8$ μm are shown in

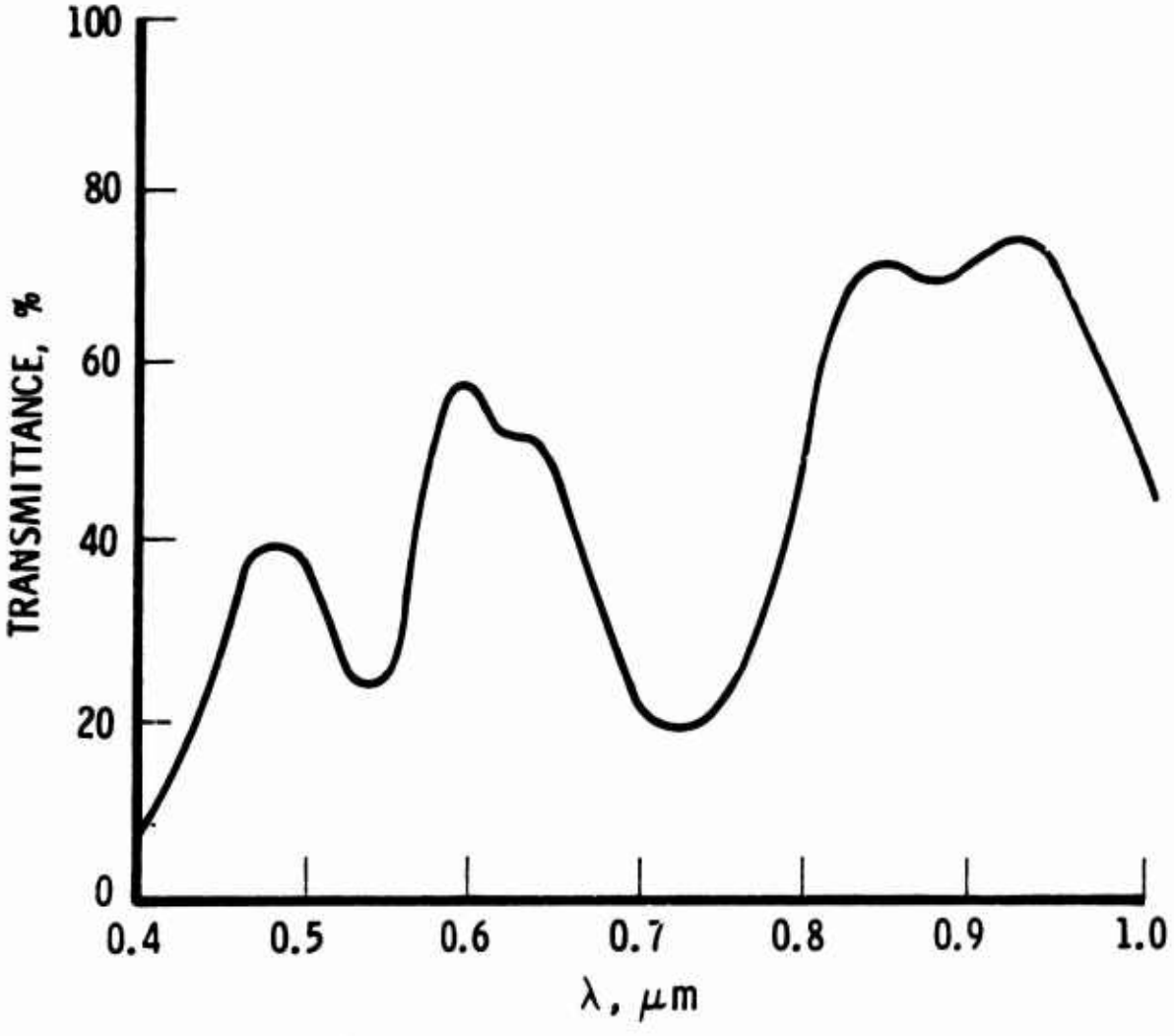

Figure 1. Calculated Transmittance T(λ) of CCI Electrode and Oxide Layers. The layers are pyroglass (0.755 μm), polysilicon (0.26 μm), and SiO_2 (0.13 μm) (Ref. 5).

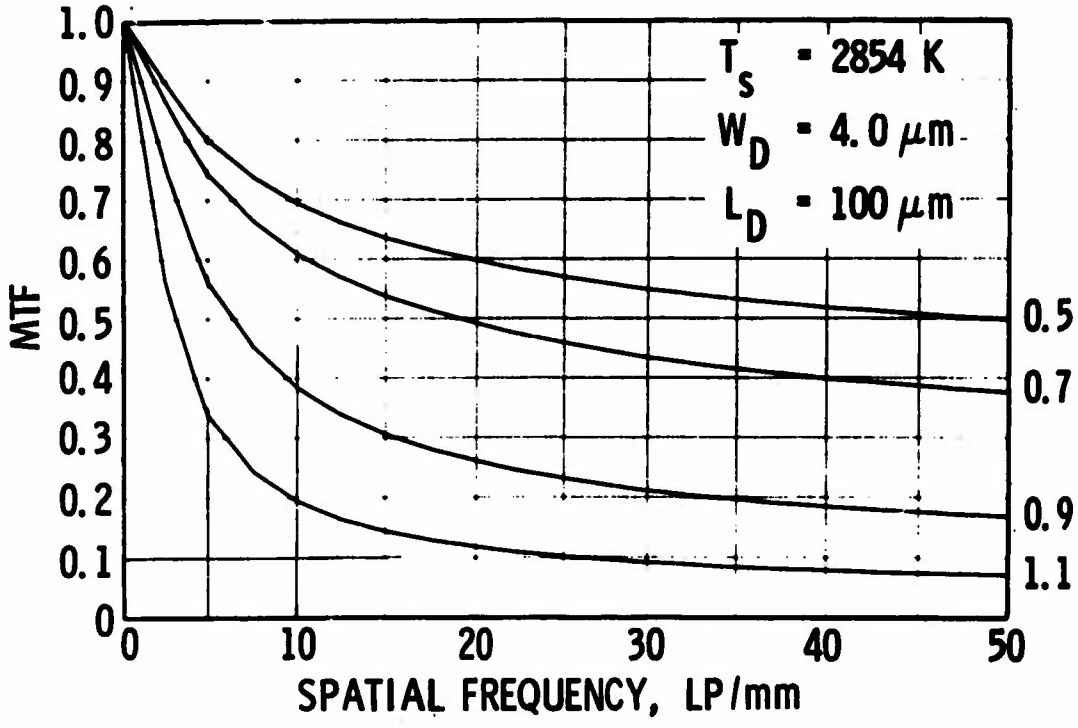

Figure 2. Broadband $\overline{MTF}$ for Frontside Illumination vs Spatial Frequency with Initial Wavelength as a Parameter. Final wavelength, 1.2 μm.

Fig. 3; they are read as described above. Comparison of Figs. 2 and 3 indicates that eliminating long wavelengths improves $\overline{MTF}$, as expected.

Calculated results for a source temperature of 4800 K and $\lambda_f = 1.2\ \mu m$ are given in Fig. 4. $\overline{MTF}$ over the band 0.5 - 1.2 μm is improved compared to Fig. 2 because of the greater number of high energy photons in the 4800 K source.

Increasing the depletion width, W_D, improves $\overline{MTF}$. This is illustrated in Fig. 5, where $\overline{MTF}$ has been calculated for $W_D = 8\ \mu m$, $T_s = 2854$ K, λ_f 1.2 μm, and all other parameters as above. For the band 0.5-1.2 μm, the improvement at 50 cycles/mm is by a factor of 1.2.

The trade-off between broadband responsivity and broadband $\overline{MTF}$ as long wavelengths are filtered from the source spectrum is indicated in Figs. 6-9. The normalized broadband responsivity is defined as:

$$R(\lambda_i, \lambda_f) = \frac{\int_{\lambda_i}^{\lambda_f} \eta(\lambda)\, N(\lambda)\, T(\lambda)\, d\lambda}{\int_{0.4}^{1.2} \eta(\lambda)\, N(\lambda)\, T(\lambda)\, d\lambda} \qquad (2)$$

For a given source, $R(\lambda_i, \lambda_f)$ gives the number of amperes created by the optical band λ_i to λ_f normalized to the number of amperes created by the entire spectral band. In Fig. 6, $R(\lambda_i, \lambda_f)$ is plotted vs λ_f with $\lambda_i = 0.4\ \mu m$ for source temperatures of 2854 K and 4800 K, and for $W_D = 4.0\ \mu m$. This quantity is greater than 0.9 for $\lambda_f \geq 0.95\ \mu m$ but decreases rapidly for $\lambda_f < 0.95\ \mu m$. The elimination of long wavelengths from the spectrum affects $\overline{MTF}$ as shown in Figs. 8 and 9. In these curves, λ_i is fixed at 0.4 μm and $\overline{MTF}$ is plotted vs λ_f with ν_s as a parameter. This is an alternative method of presenting some of the same information contained in Figs. 2-4. As an example, if $\overline{MTF}$ is desired for the band 0.4-0.9 μm, locate 0.9 μm on the

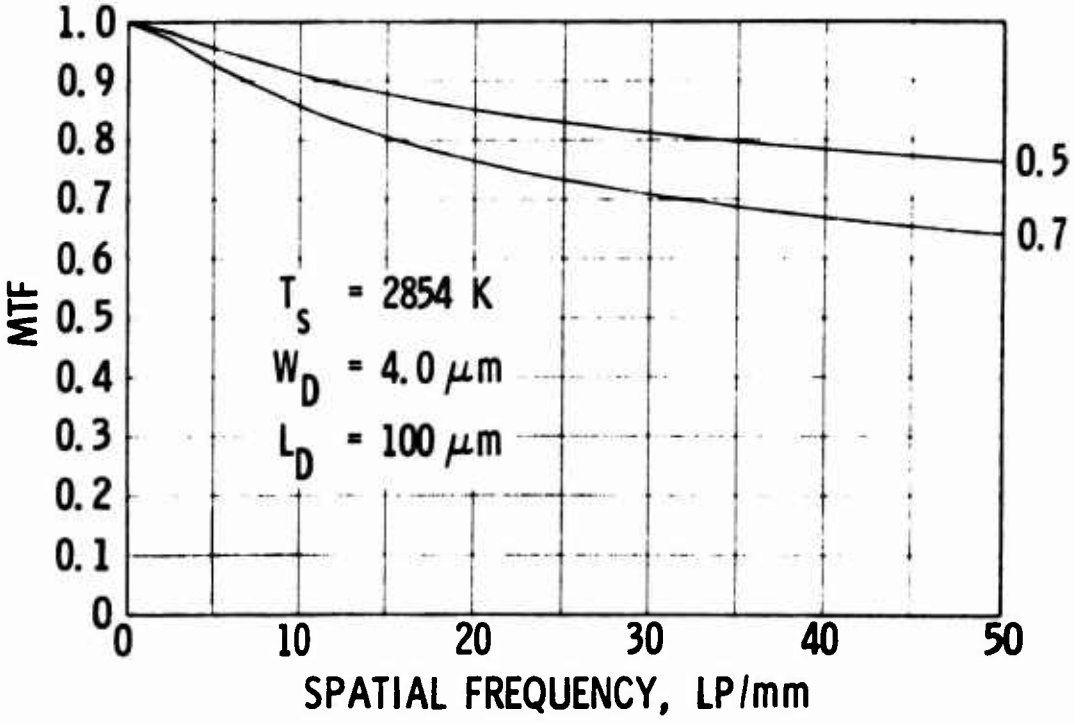

Figure 3. $\overline{\text{MTF}}$ for Frontside Illumination vs Spatial Frequency with Initial Wavelength as a Parameter. Final wavelength, 0.8 μm.

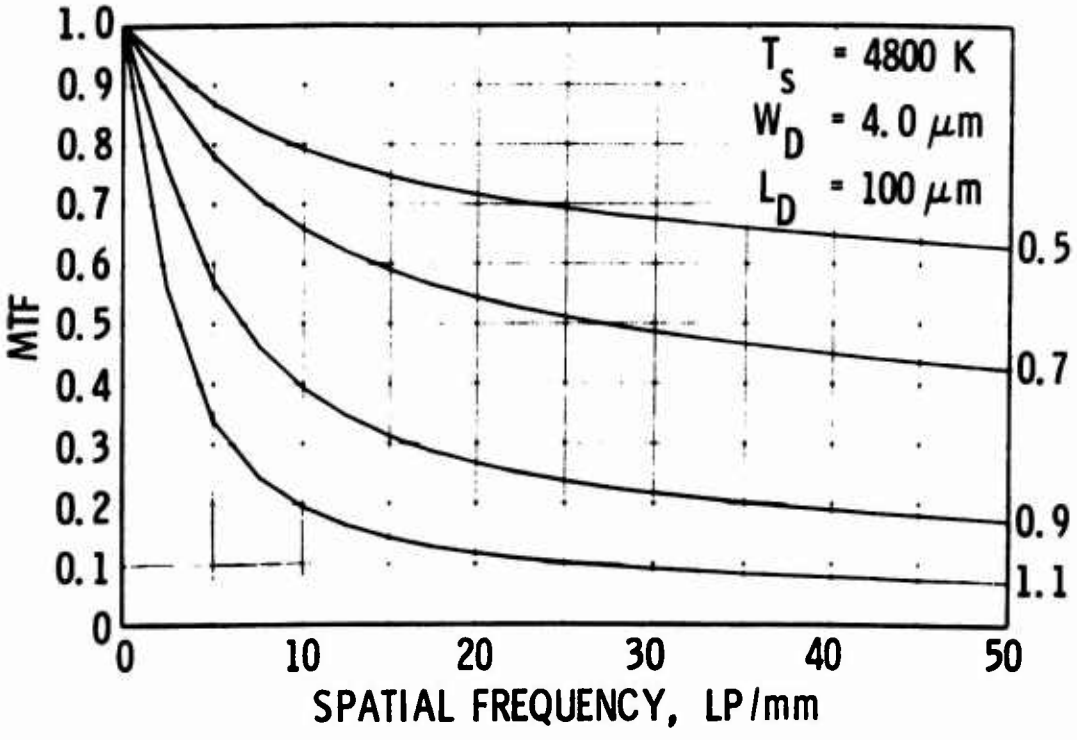

Figure 4. $\overline{MTF}$ for Frontside Illumination vs Spatial Frequency with Initial Wavelength as a Parameter. Final wavelength, 1.2 μm.

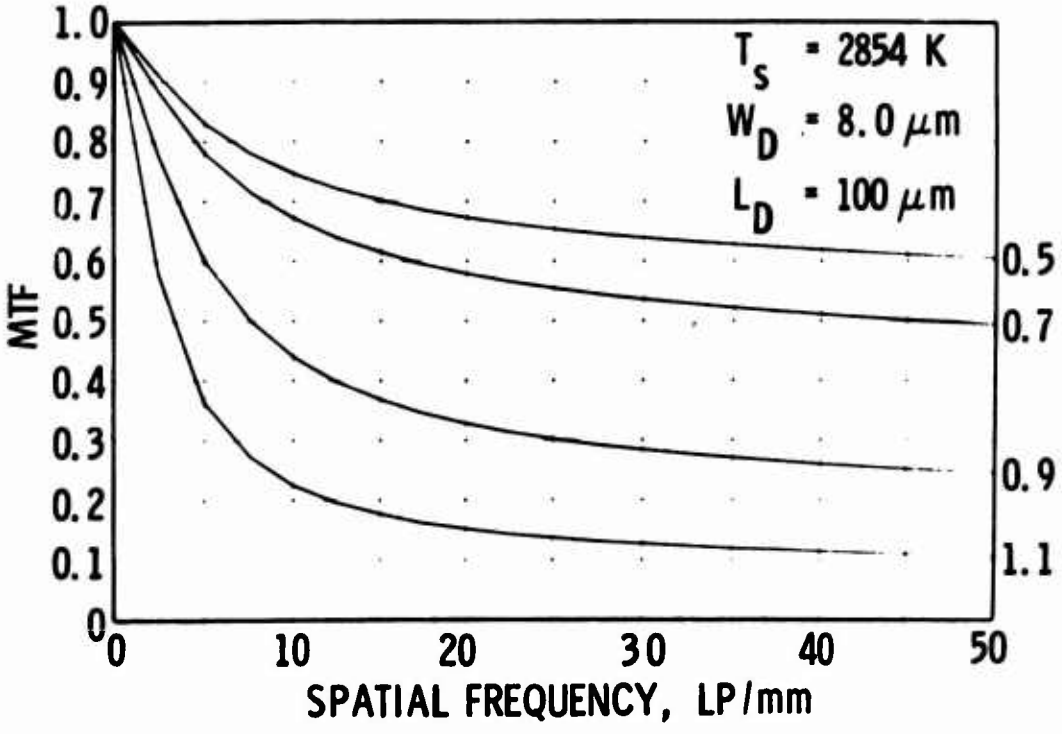

Figure 5. $\overline{MTF}$ for Frontside Illumination vs Spatial Frequency with Initial Wavelength as a Parameter. Final wavelength, 1.2 μm. W_D = 8.0 μm to indicate the effect of increasing the depletion width.

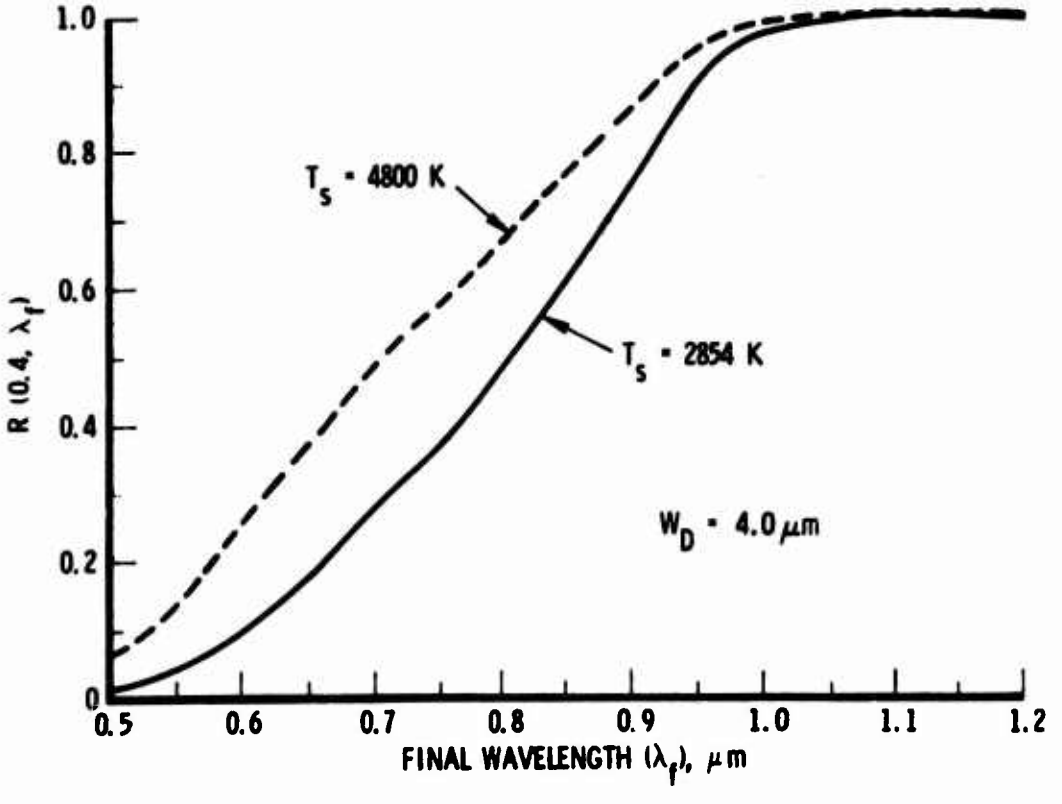

Figure 6. Normalized Broadband Responsivity vs Final Wavelength for Initial Wavelength of 0.4 μm and Frontside Illumination.

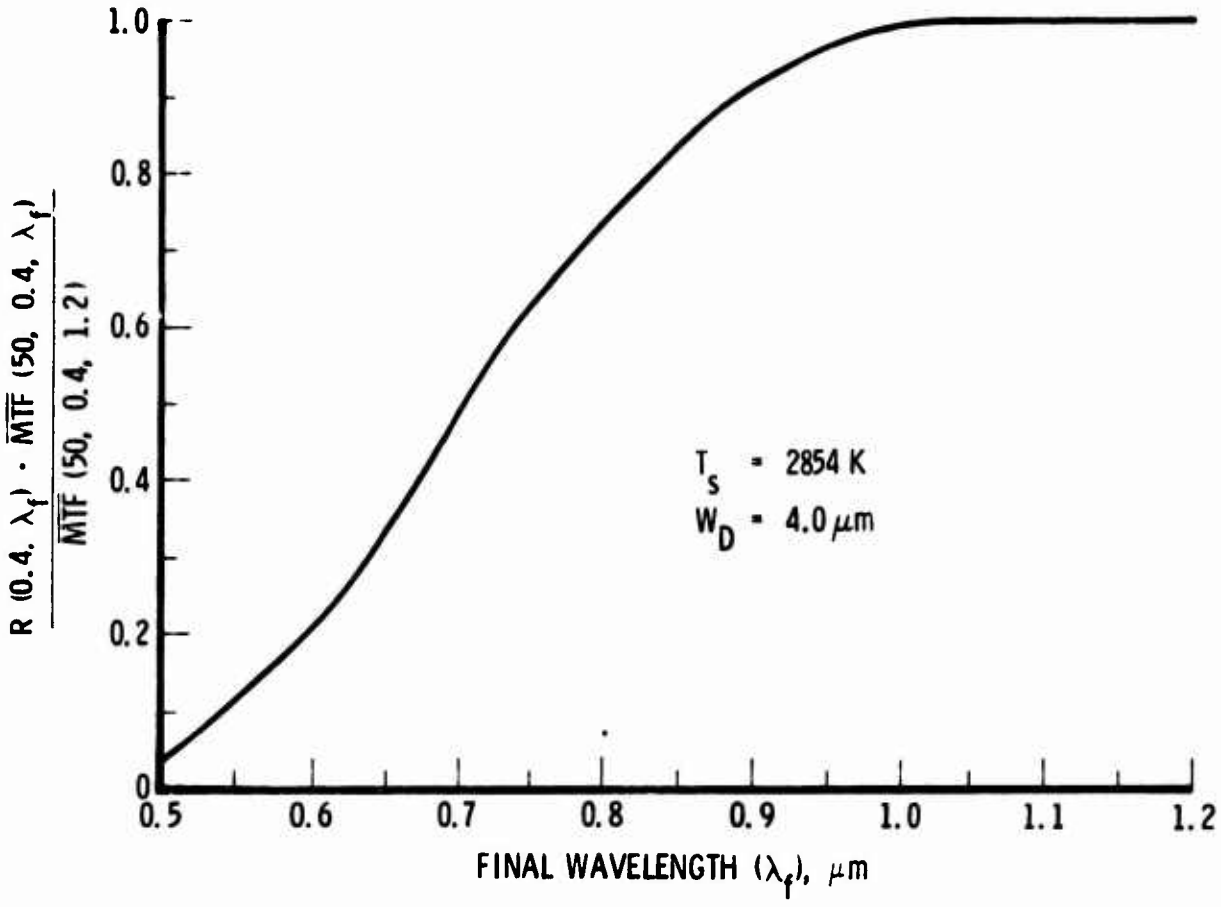

Figure 7. Normalized Broadband Responsivity Times Normalized Broadband $\overline{MTF}$ at 50 cycles/mm vs Final Wavelength for Initial Wavelength of 0.4 μm.

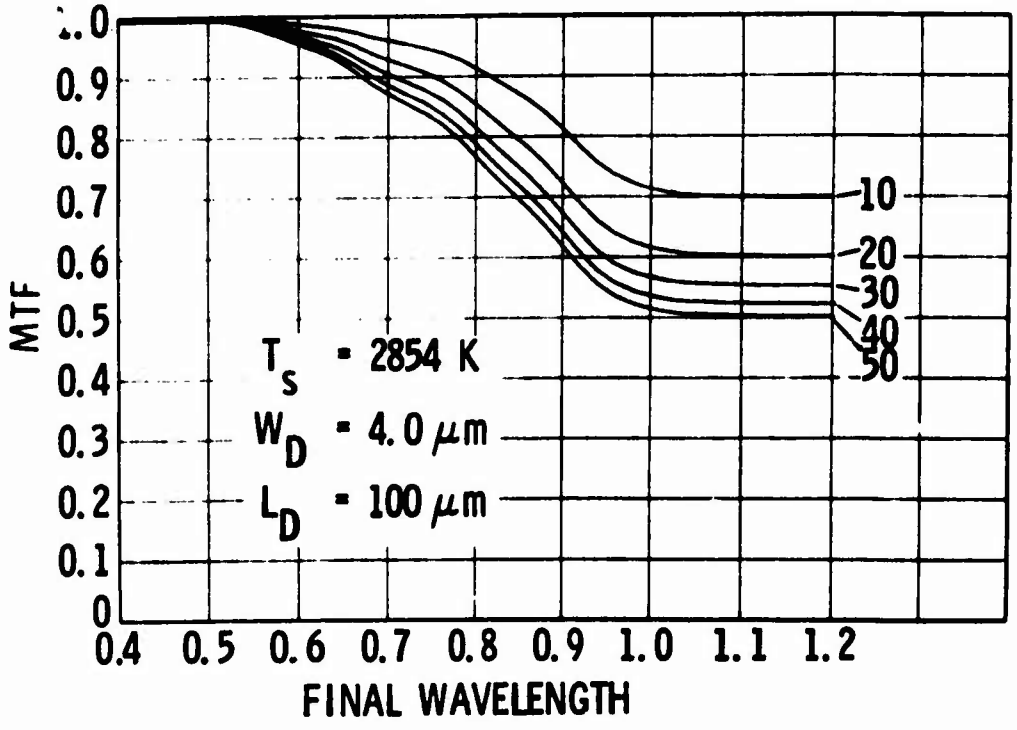

Figure 8. Broadband $\overline{MTF}$ for Frontside Illumination vs Final Wavelength with Spatial Frequency as a Parameter. Initial wavelength, 0.4 μm; T_s, 2854 K.

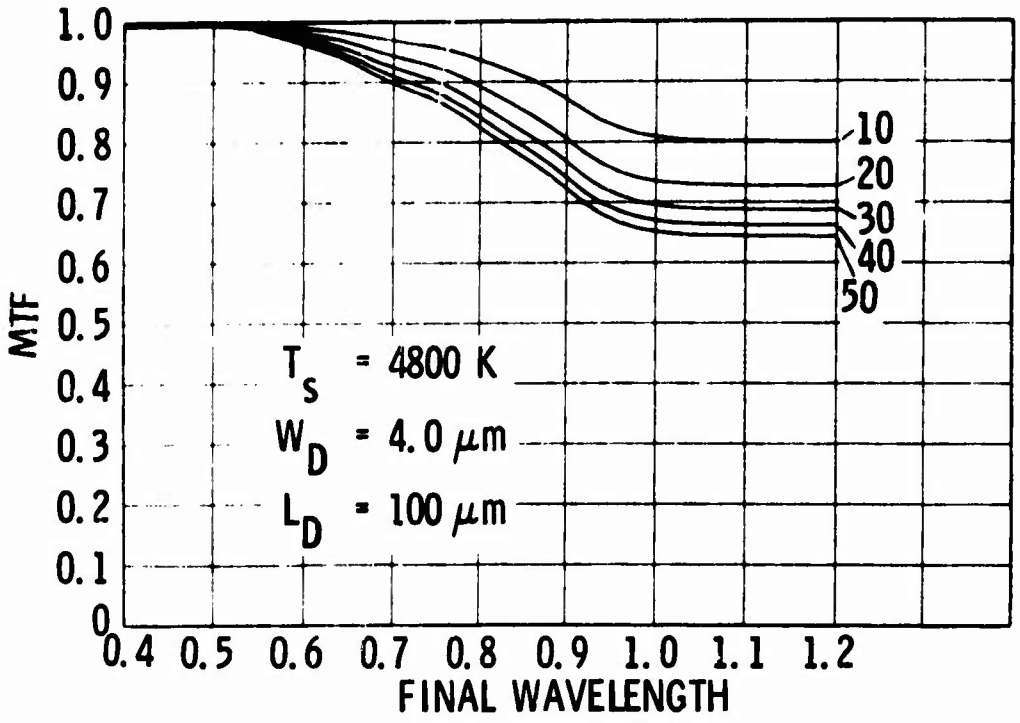

Figure 9. Broadband $\overline{MTF}$ for Frontside Illumination vs Final Wavelength with Spatial Frequency as a Parameter. Initial wavelength, 0.4 μm; T_s, 4800 K.

horizontal-axis and read $\overline{MTF}$ at 50, 40....10 cycles/mm where the vertical line passing through 0.9 μm intersects the plotted curves.

Whether filtering of long wavelengths actually improves overall imager performance is dependent upon the product of broadband responsivity and $\overline{MTF}$. In Fig. 7, the product $R(0.4, \lambda_f) \cdot \overline{MTF}\,(50, 0.4, \lambda_f) / \overline{MTF}\,(50, 0.4, 1.2)$ is plotted vs λ_f. This quantity is a measure of the total signal strength obtained for a spatial frequency of 50 cycles/mm as λ_f is varied. It never exceeds 1.0, indicating that imager performance with respect to carrier diffusion effects is not improved by filtering out long wavelengths. This results because responsivity falls more rapidly than $\overline{MTF}$ increases as the optical band is restricted. The final wavelength can be restricted to ~0.95 μm for $T_s = 2854$ K with less than 5% loss in performance, however. The same conclusions hold for other source temperatures and depletion widths. The ability to restrict the optical band without degrading imager performance may be beneficial to the overall system performance. For instance, lens performance might be improved by eliminating long wavelengths and any difficulties associated with maintaining focus over a broad optical spectrum would be lessened.

IV. BACKSIDE ILLUMINATION

To evaluate MTF for backside illuminated CCI's the parameters W_D = 4.0 μm, L_D = 100 μm, and T_W = wafer thickness = 10.0 μm (Ref. 4) are chosen. In addition, to evaluate $T(\lambda) = 1-R(\lambda)$, values of reflectivity for a clean silicon surface are used (Ref. 3). Curves of $\overline{MTF}$ vs ν_s with λ_i as a parameter are shown in Figs. 10 and 11 for T_s = 2854 K and 4800 K, respectively. In these curves, λ_f is fixed at 1.2 μm. As expected, elimination of short wavelengths improves $\overline{MTF}$.

The effect of increasing the depletion width to 8.0 μm, with all other parameters remaining the same, is to practically eliminate all $\overline{MTF}$ degradation caused by carrier diffusion. This is illustrated in Fig. 12, where $\overline{MTF}$ is shown for W_D = 8.0 μm, T_s = 4800 K, and λ_f = 1.2 μm.

The trade-off between quantum efficiency and $\overline{MTF}$ is given in Figs. 13-16 for the backside illuminated imager considered (W_D = 4.0 μm). In Fig. 13 $R(\lambda_i, 1.2)$, from Eq. (2), is plotted vs λ_i; these curves therefore indicate how normalized responsivity falls off as short wavelengths are filtered from the source spectrum. Figures 15 and 16 show $\overline{MTF}$ as a function of λ_i for T_s = 2854 K and 4800 K (λ_f = 1.2 μm). Finally, the product $R(\lambda_i, 1.2) \cdot \overline{MTF}(50, \lambda_i, 1.2) / \overline{MTF}(50, 0.4, 1.2)$ is given in Fig. 14. As in the case of the frontside illuminated imager, this quantity never exceeds 1.0 indicating that the best imager performance is obtained for the full 0.4-1.2 μm optical band.

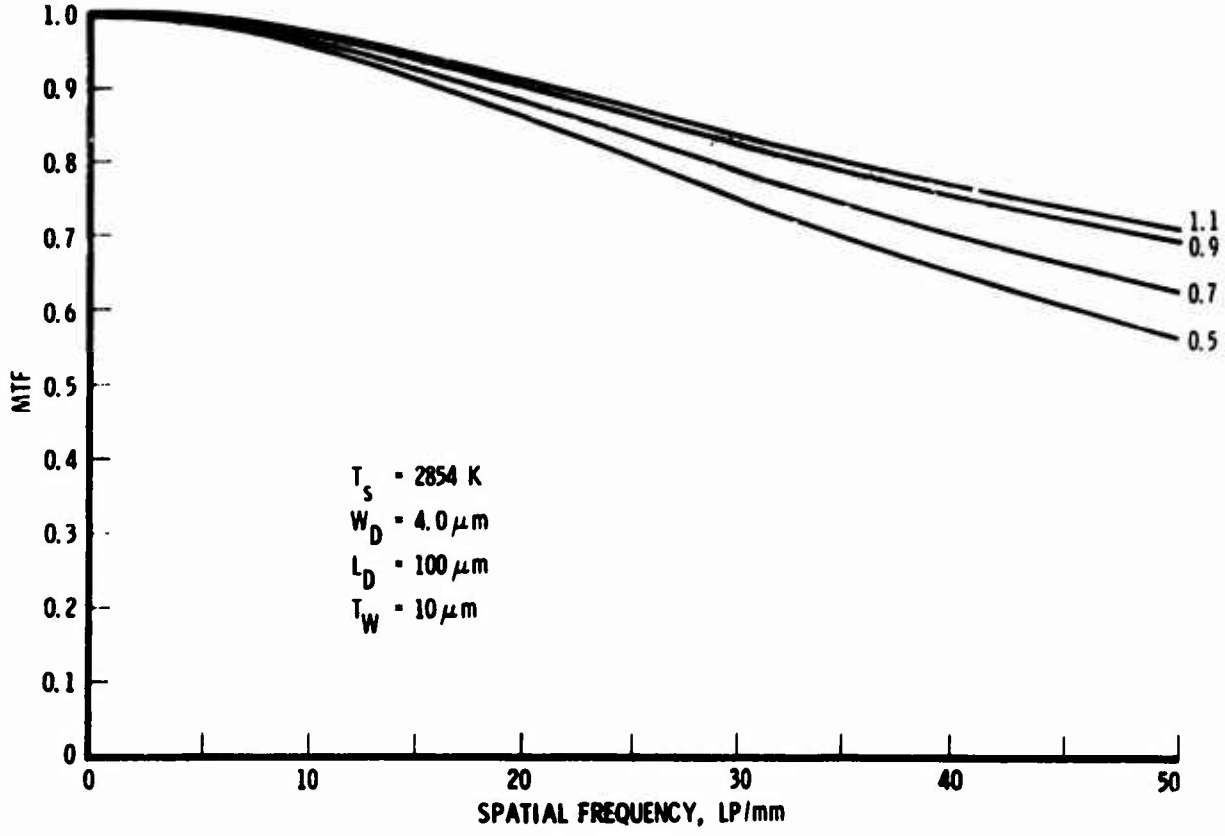

Figure 10. Broadband $\overline{\text{MTF}}$ for Backside Illumination vs Spatial Frequency with Initial Wavelength as a Parameter. Final wavelength, 1.2 μm; T_s, 2854 K.

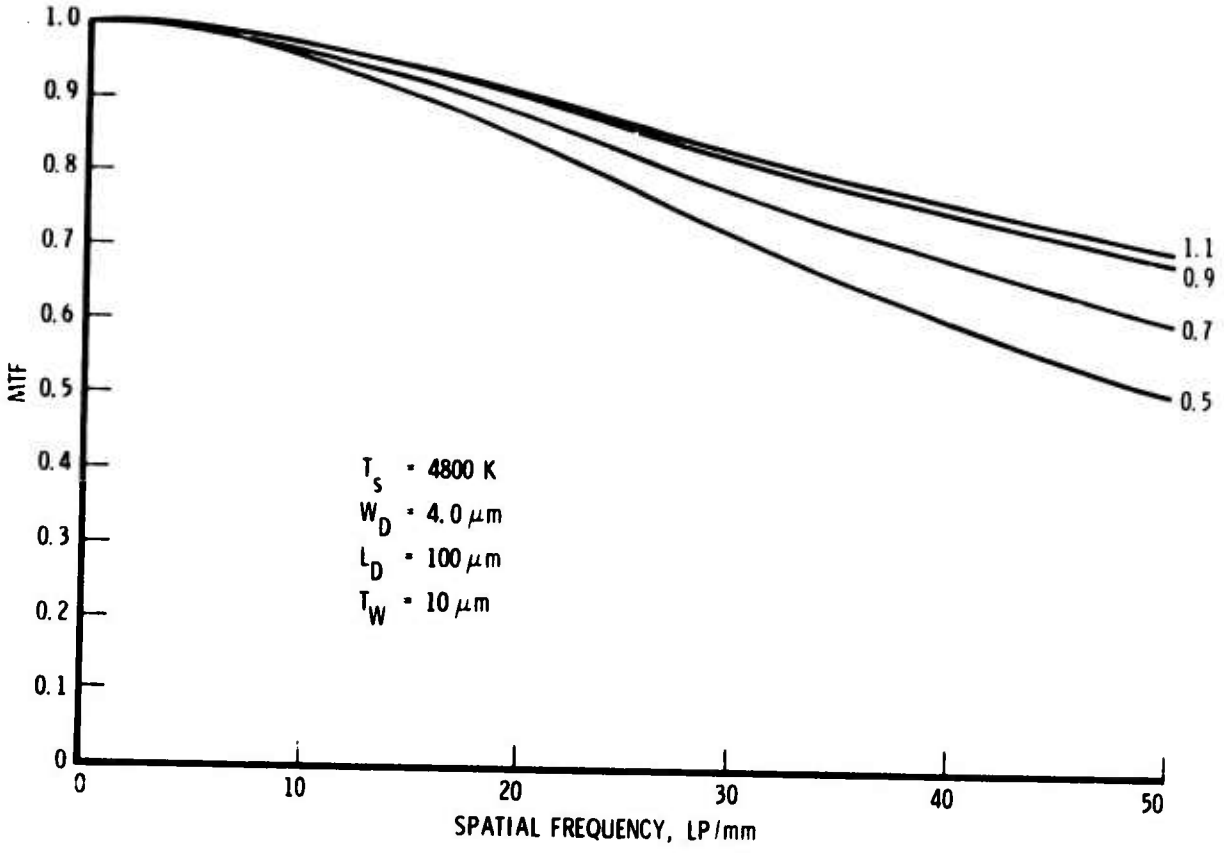

Figure 11. Broadband $\overline{MTF}$ for Backside Illumination vs Spatial Frequency with Initial Wavelength as a Parameter. Final wavelength, 1.2 μm; T_s, 4800 K.

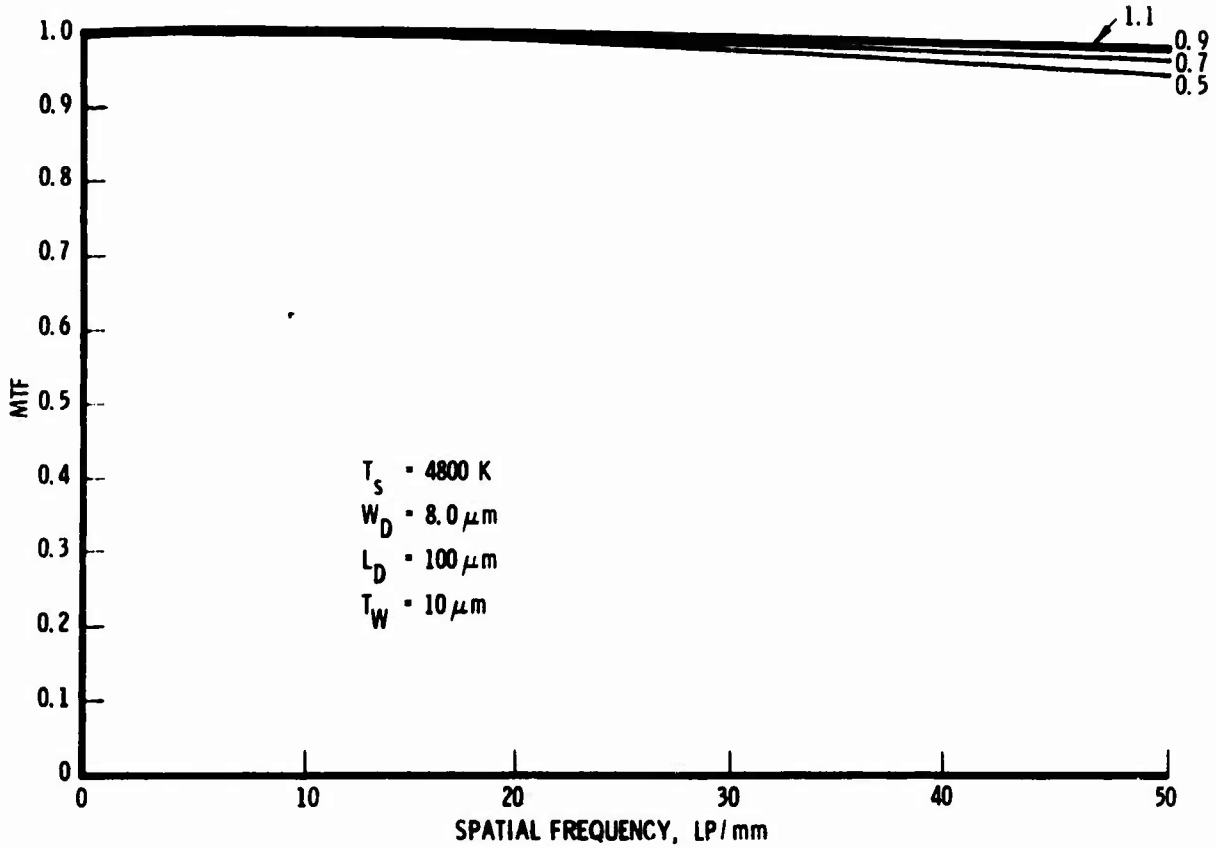

Figure 12. Broadband $\overline{MTF}$ for Backside Illumination vs Spatial Wavelength with Initial Wavelength as a Parameter. Final wavelength, 1.2 μm; T_s, 4800 K; W_D, 8.0 μm.

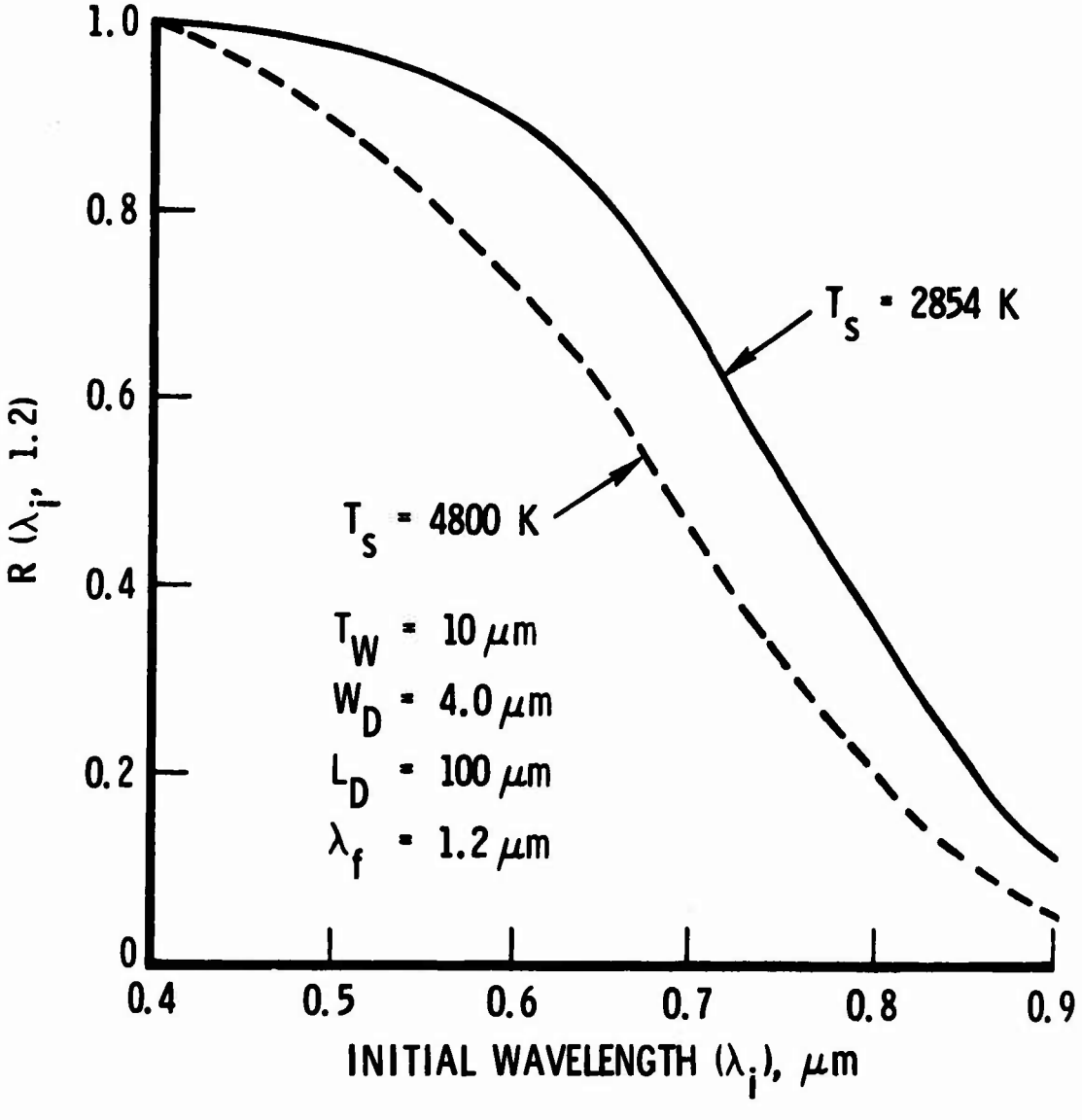

Figure 13. Normalized Broadband Responsivity vs Initial Wavelength for Final Wavelength of 1.2 μm and Backside Illumination

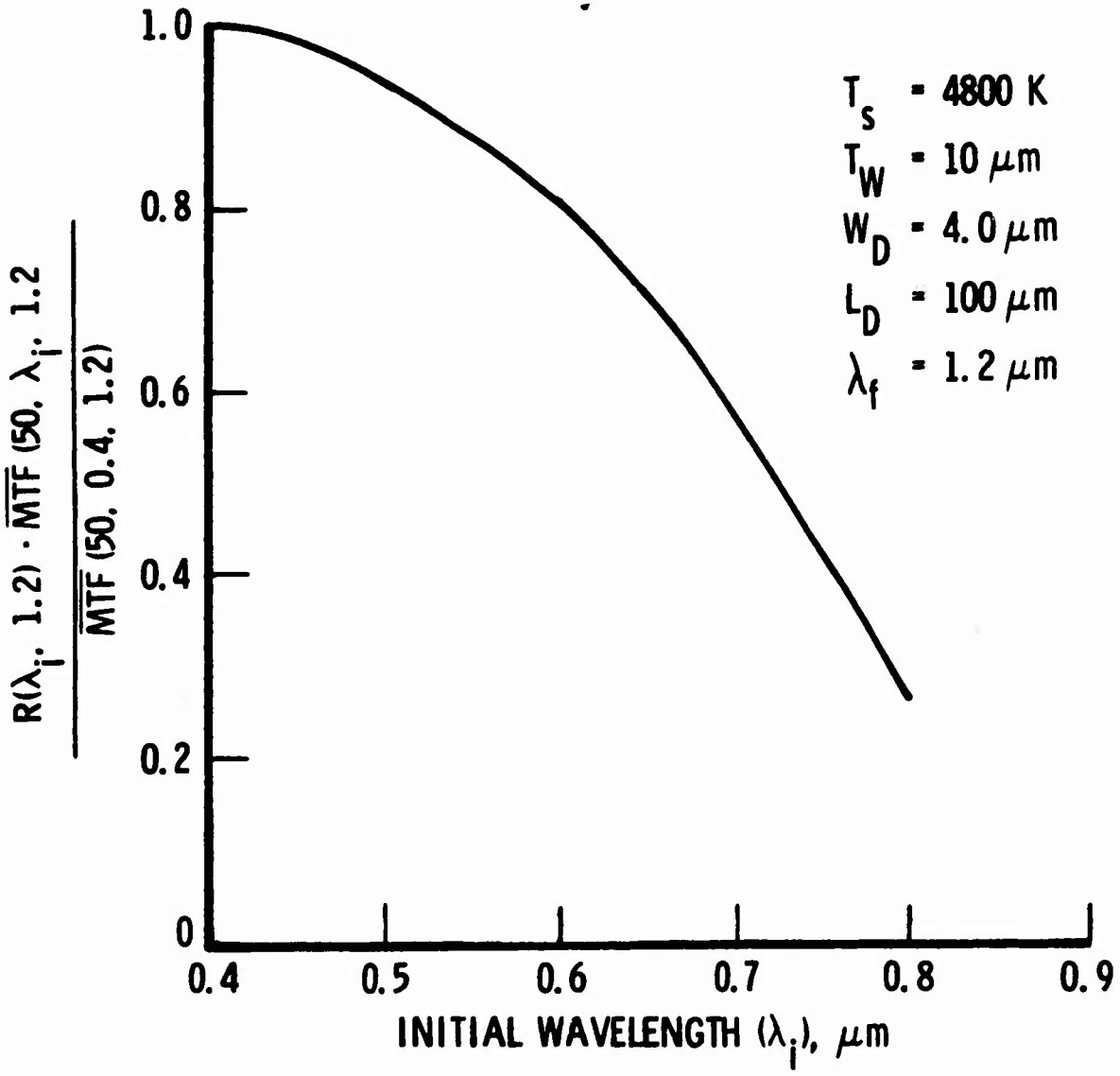

Figure 14. Normalized Broadband Responsivity Times Normalized Broadband $\overline{MTF}$ at 50 cycles/mm vs Initial Wavelength for Final Wavelength of 1.2 μm.

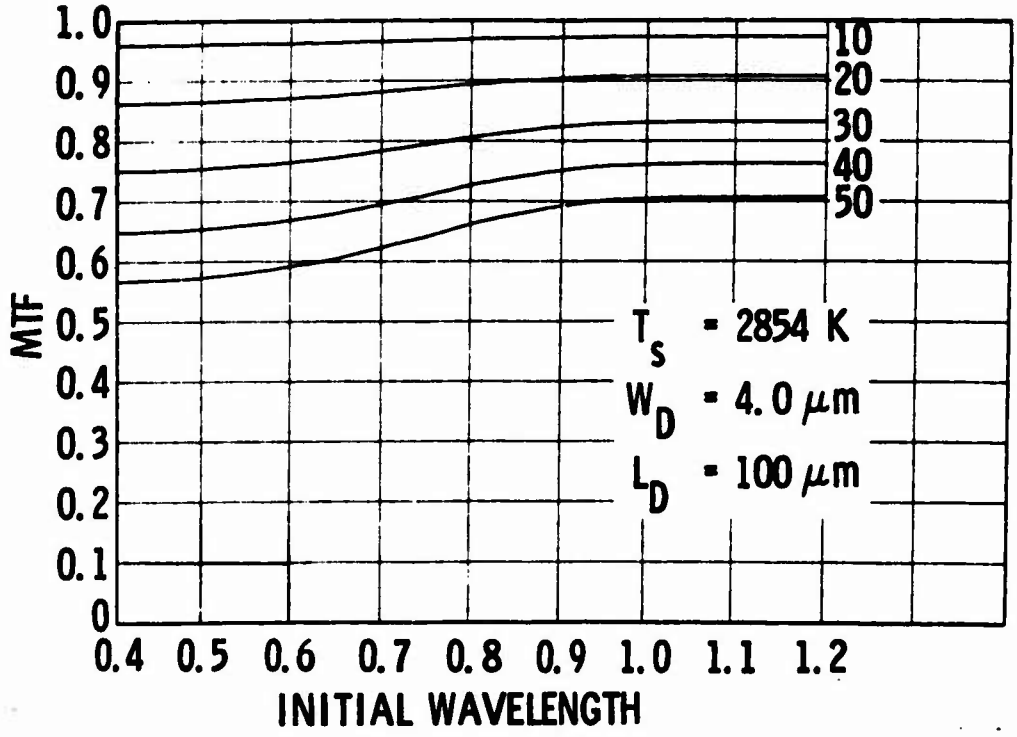

Figure 15. Broadband $\overline{MTF}$ for Backside Illumination vs Initial Wavelength with Spatial Frequency as a Parameter. Final wavelength, 1.2 μm; T_s, 2854 K.

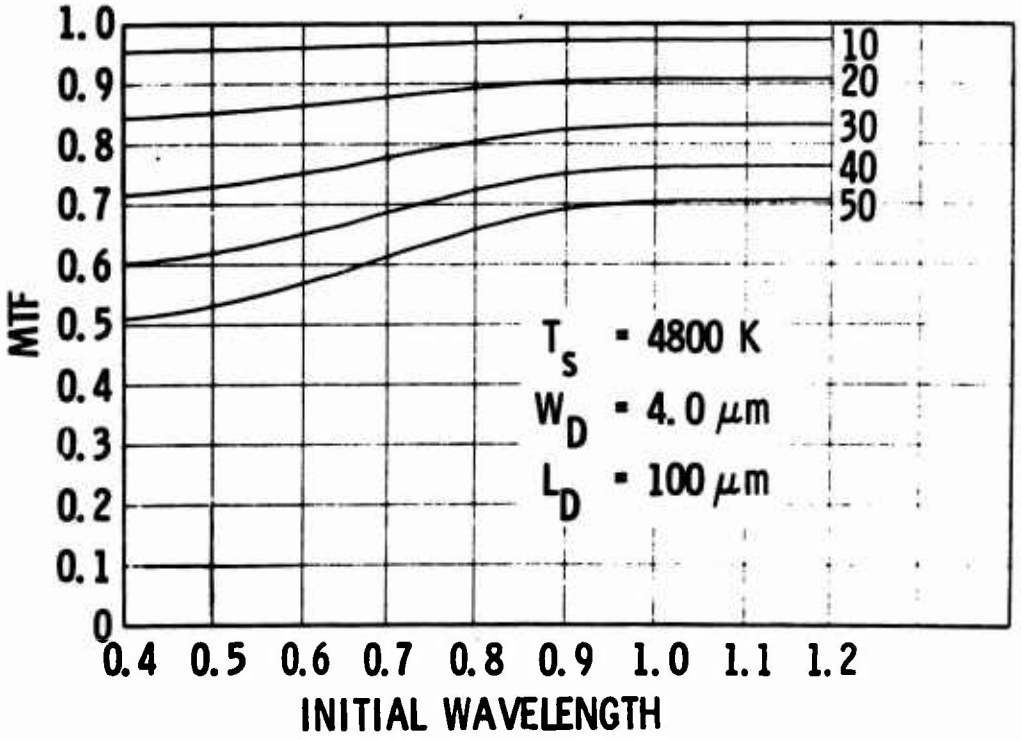

Figure 16. Broadband $\overline{MTF}$ for Backside Illumination vs Initial Wavelength with Spatial Frequency as a Parameter. Final wavelength, 1.2 μm; T_s, 4800 K.

V. DISCUSSION

The calculated results discussed above indicate that even though $\overline{MTF}$ (ν_s, λ) for a charge coupled imager may become small for high spatial frequencies and certain wavelengths (Ref. 1), when broadband excitation is considered $\overline{MTF}$ can be reasonably high. This is due to the fact that the wavelengths which contribute most to carrier diffusion degradation (short and long wavelengths for back- and frontside illumination respectively) contribute only a small fraction of the total response for the source temperatures chosen. Comparison of Figs. 2, 4, and 10, 11 indicates that for $W_D = 4.0$ μm and full band the backside illuminated device has somewhat better $\overline{MTF}$. If the depletion width is increased to 8.0 μm, the backside illuminated imager is considerably better in terms of $\overline{MTF}$ than the frontside illuminated device (Figs. 5 and 12). Note that increasing the depletion width also is beneficial in both types of devices in increasing the responsivity. $\overline{MTF}$ for the frontside illuminated device might be improved somewhat by thinning the wafer and creating a high recombination velocity back surface in order to capture carriers created far from the depletion region. This is essentially like filtering out the long wavelengths – improvement in $\overline{MTF}$ is obtained at the expense of responsivity. (Thinning a frontside illuminated device to the same thickness, ≈10 μm, as a backside illuminated device would of course result in comparable values of $\overline{MTF}$. However the responsivity of the frontside illuminated device would be less due to the transmission of the oxide-electrode layers.) It therefore appears that, from the standpoint of best broadband modulation transfer function due to carrier diffusion effects, the backside approach to charge coupled imager fabrication is the most advantageous.

REFERENCES

1. D. H. Seib, "Carrier Diffusion Degradation of Modulation Transfer Function in Charge Coupled Imagers", IEEE Trans. on Elect. Dev., Vol. ED-21, pp. 210-217, March, 1974.

2. M. H. Crowell and E. F. Labuda, "The Silicon Diode Array Camera Tube," Bell Syst. Tech. J., Vol. 48, pp. 1481-1528, 1969.

3. R. C. Eden, Ph. D. Dissertation, Stanford University, 1967 (unpublished).

4. G. A. Antcliffe, L. J. Hornbeck, J. M. Younse, J. B. Barton, and D. R. Collins, "Large-Area CCD Imagers for Spacecraft Applications", Proc. Symp on Charged Coupled Device Technology for Scientific Applications, March 6-7, 1975, Jet Propulsion Laboratory, Calif. Inst. of Tech., Pasadena, California 91103, pp. 125-136.

5. R. W. Brown and S. G. Chamberlain, "Quantum Efficiency of a Silicon Gate Charged-Coupled Optical Imaging Array", Phys. Stat. Sol. (a) Vol. 20, pp. 675-685.

LABORATORY OPERATIONS

The Laboratory Operations of The Aerospace Corporation is conducting experimental and theoretical investigations necessary for the evaluation and application of scientific advances to new military concepts and systems. Versatility and flexibility have been developed to a high degree by the laboratory personnel in dealing with the many problems encountered in the nation's rapidly developing space and missile systems. Expertise in the latest scientific developments is vital to the accomplishment of tasks related to these problems. The laboratories that contribute to this research are:

Aerophysics Laboratory: Launch and reentry aerodynamics, heat transfer, reentry physics, chemical kinetics, structural mechanics, flight dynamics, atmospheric pollution, and high-power gas lasers.

Chemistry and Physics Laboratory: Atmospheric reactions and atmospheric optics, chemical reactions in polluted atmospheres, chemical reactions of excited species in rocket plumes, chemical thermodynamics, plasma and laser-induced reactions, laser chemistry, propulsion chemistry, space vacuum and radiation effects on materials, lubrication and surface phenomena, photosensitive materials and sensors, high precision laser ranging, and the application of physics and chemistry to problems of law enforcement and biomedicine.

Electronics Research Laboratory: Electromagnetic theory, devices, and propagation phenomena, including plasma electromagnetics; quantum electronics, lasers, and electro-optics; communication sciences, applied electronics, semiconducting, superconducting, and crystal device physics, optical and acoustical imaging; atmospheric pollution; millimeter wave and far-infrared technology.

Materials Sciences Laboratory: Development of new materials; metal matrix composites and new forms of carbon; test and evaluation of graphite and ceramics in reentry; spacecraft materials and electronic components in nuclear weapons environment; application of fracture mechanics to stress corrosion and fatigue-induced fractures in structural metals.

Space Physics Laboratory: Atmospheric and ionospheric physics, radiation from the atmosphere, density and composition of the atmosphere, aurorae and airglow; magnetospheric physics, cosmic rays, generation and propagation of plasma waves in the magnetosphere; solar physics, studies of solar magnetic fields; space astronomy, x-ray astronomy; the effects of nuclear explosions, magnetic storms, and solar activity on the earth's atmosphere, ionosphere, and magnetosphere; the effects of optical, electromagnetic, and particulate radiations in space on space systems.

THE AEROSPACE CORPORATION
El Segundo, California

• • •